PDMP Blocks Brefeldin A–induced Retrograde Membrane Transport from Golgi to ER: Evidence for Involvement of Calcium Homeostasis and Dissociation from Sphingolipid Metabolism

Jan Willem Kok,* Teresa Babia,§ Catalin M. Filipeanu,‡ Adriaan Nelemans,‡ Gustavo Egea,§ and Dick Hoekstra*

*Department of Physiological Chemistry, ‡Department of Clinical Pharmacology, University of Groningen, Groningen Institute for Drug Studies (GIDS), 9713 AV Groningen, The Netherlands; and §Universitat de Barcelona, Facultat de Medicina, Departament de Biologia Cellular, Institut d'Investigacions Biomediques August Pi I Sunyer, 08036 Barcelona, Spain

Abstract. In this study, we show that an inhibitor of sphingolipid biosynthesis, D,L-*threo*-1-phenyl-2-decanoylamino-3-morpholino-1-propanol (PDMP), inhibits brefeldin A (BFA)-induced retrograde membrane transport from Golgi to endoplasmic reticulum (ER). If BFA treatment was combined with or preceded by PDMP administration to cells, disappearance of discrete Golgi structures did not occur. However, when BFA was allowed to exert its effect before PDMP addition, PDMP could not "rescue" the Golgi compartment.

Evidence is presented showing that this action of PDMP is indirect, which means that the direct target is not sphingolipid metabolism at the Golgi apparatus. A fluorescent analogue of PDMP, 6-(*N*-[7-nitro-2,1,3-benzoxadiazol-4-yl]amino)hexanoyl-PDMP (C_6-NBD-PDMP), did not localize in the Golgi apparatus. Moreover, the effect of PDMP on membrane flow did not correlate with impaired C_6-NBD-sphingomyelin biosynthesis and was not mimicked by exogenous C_6-ceramide addition or counteracted by exogenous C_6-glucosylceramide addition. On the other hand, the PDMP effect was mimicked by the multidrug resistance protein inhibitor MK571.

The effect of PDMP on membrane transport correlated with modulation of calcium homeostasis, which occurred in a similar concentration range. PDMP released calcium from at least two independent calcium stores and blocked calcium influx induced by either extracellular ATP or thapsigargin. Thus, the biological effects of PDMP revealed a relation between three important physiological processes of multidrug resistance, calcium homeostasis, and membrane flow in the ER/Golgi system.

Key words: ceramide • retrograde membrane flow • β-COP • multidrug resistance • intracellular calcium

D,L-*THREO*-1-PHENYL-2-DECANOYLAMINO-3-MORPHOLINO-1-PROPANOL (PDMP)[1] is a well-known inhibitor of sphingolipid biosynthesis (Radin et al., 1993). The formation of glucosylceramide (GlcCer) is drastically inhibited by PDMP, while the effect on sphingomyelin biosynthesis appears to depend on the cell type and the concentration of the drug. In addition, PDMP treatment may lead to an accumulation of the endogenous sphingolipid precursor ceramide (Cer).

Apart from its effect on sphingolipid synthesis, PDMP has been shown to inhibit anterograde membrane transport through the Golgi complex and from the Golgi complex to the plasma membrane (Rosenwald et al., 1992). A similar effect was observed when cells were incubated with a short-chain analogue of Cer, C_6-Cer (Rosenwald and Pagano, 1993). This suggests that PDMP-induced inhibition of anterograde membrane transport may (in part) be a result of an elevation of the intracellular Cer level.

In this study, we investigated the effect of PDMP on brefeldin A (BFA)-induced retrograde membrane transport from Golgi to ER. The formation of transport vesicles involved in retrograde trafficking, as well as anterograde, has been extensively studied at the molecular level (Aridor and Balch, 1996; Bednarek et al., 1996). Assembly of

Address all correspondence to J.W. Kok, Department of Physiological Chemistry, University of Groningen, Groningen Institute for Drug Studies (GIDS), A. Deusinglaan 1, 9713 AV Groningen, The Netherlands. Tel.: 31-(0)50-3632725. Fax: 31-(0)50-3632728. E- mail: j.w.kok@med.rug.nl

1. *Abbreviations used in this paper*: BFA, brefeldin A; Cer, ceramide; C_6-NBD, 6-(*N*-[7-nitro-2,1,3-benzoxadiazol-4-yl]amino)hexanoyl or hexanoic acid; GlcCer, glucosylceramide; ManII, mannosidase II; MDR, multidrug resistance; MRP, multidrug resistance protein; NRK, normal rat kidney; PDMP, D,L-*threo*-1-phenyl-2-decanoylamino-3-morpholino-1-propanol; P-gp, P-glycoprotein; SM, sphingomyelin.

coats is thought to provide the driving force for vesicle budding. Two distinct vesicle coats, COPI and COPII, are involved in retrograde and anterograde trafficking, respectively. COPI, a cytosolic protein consisting of seven subunits, is recruited to the target membrane after activation and binding of the small GTP-binding protein ARF1. Treatment of cells with BFA is known to interfere with coat assembly (Scheel et al., 1997) and results in retrograde merging of Golgi membranes with the ER (Lippincott et al., 1989; Klausner et al., 1992). BFA blocks the assembly of coated vesicles by inhibiting GTP/GDP exchange on ARF1 (Donaldson et al., 1992; Helms and Rothman, 1992), thus preventing the binding of ARF and coatomer to Golgi membranes. Golgi membrane tubulation and absorption into the ER follows COPI dissociation from membranes (Sciaky et al., 1997). It is assumed that this proceeds via direct (i.e., uncoupled from vesicle budding) fusion reactions between Golgi membranes as well as between Golgi and ER membranes (Elazar et al., 1994). ARF and coatomer thus prevent direct fusion between membranes and provide a molecular mechanism for controlled transfer of cargo between compartments through vesicular carriers. In line with this, coat disassembly occurs before fusion with the target membrane when ARF is triggered to hydrolyze bound GTP (Tanigawa et al., 1993). It is not known whether uncoupled fusion occurs physiologically, i.e., without BFA, but it is not likely to be involved in signal-dependent retrograde transport of KDEL-bearing proteins from (the plasma membrane via) the Golgi to the ER (Johannes et al., 1997; Cole et al., 1998). In this study, we show that PDMP inhibits the disassembly of the Golgi complex and its merging with the ER compartment in BFA-treated cells. This was assessed by staining of the Golgi apparatus using two approaches. One involved Golgi staining in fixed cells, using antibodies to a *cis*-Golgi resident protein, mannosidase II (ManII), and a *trans*-Golgi resident protein, $GMP_{t\text{-}1}$ (Alcalde et al., 1992, 1994). The other approach involved the use of 6-(*N*-[7-nitro-2,1,3-benzoxadiazol-4-yl]amino)hexanoyl-Cer (C_6-NBD-Cer), a well-known Golgi marker (Lipsky and Pagano, 1985; Pagano, 1989), which offers the advantage of studying Golgi morphology in intact, living cells. Furthermore, sphingolipid metabolism can be monitored concomitantly, since in the Golgi conversion of C_6-NBD-Cer to C_6-NBD-sphingomyelin (SM) and C_6-NBD-glycolipids occurs. We conclude that PDMP inhibits BFA-induced retrograde Golgi to ER membrane flow in various cell types, since both newly synthesized sphingolipids and Golgi resident proteins were retained in discrete Golgi structures in BFA-treated cells. Evidence is provided for an indirect mechanism of action of PDMP, involving modulation of calcium homeostasis and interaction with multidrug resistance (MDR) proteins.

Materials and Methods

Materials

D-sphingosine, BFA, cyclosporin A, thapsigargin, and E3A5 mouse monoclonal anti–β-COP antibody were obtained from Sigma Chemical Co. (St. Louis, MO). The succinimidyl ester of C_6-NBD. Bodipy™-503/512-C_5, and indo-1-HS/AM were from Molecular Probes (Eugene, OR). PDMP, D,L-*threo*-lyso-PDMP, C_6-Cer, and 1-β-D-glucosylsphingosine were purchased from Matreya, Inc. (Pleasant Gap, PA). TRITC/FITC anti–rabbit/mouse IgG $F(ab')_2$ fragments and ATP were from Boehringer Mannheim GmbH (Mannheim, Germany). MK571 and PSC833 were kind gifts from Dr. E. Vellenga (University of Groningen, the Netherlands). Anti-ManII polyclonal antibodies were kindly provided by Dr. A. Velasco (University of Sevilla, Spain), and anti-$GMP_{t\text{-}1}$ antibodies were provided by Dr. I. Sandoval (Centro de Biologia Molecular Severo Ochoa, Consejo Superior de Investigaciones Cientificas, Universidad Autonoma de Madrid, Spain).

Cell Culture

Monocultures of HT29 G+ or normal rat kidney (NRK) cells were grown in Dulbecco's minimal essential medium (DME, containing 25 mM glucose), supplemented with 10% (vol/vol) decomplemented (56°C, 30 min) FCS, in a water-saturated atmosphere of 5% CO_2/95% air. During the exponential phase of growth, the culture medium was changed every 48 h. For maintenance purposes, cells were trypsinized once (HT29) or twice (NRK) a week and plated at appropriate densities to obtain confluent layers after 1 wk of culture.

C_6-(NBD-)sphingolipid Synthesis and Incubation Conditions

(Fluorescent) short-chain sphingolipids/PDMP were synthesized according to Kok and Hoekstra (1993). C_6-NBD-Cer and C_6-NBD-PDMP were synthesized from D-*erythro*-sphingosine and D,L-*threo*-lyso-PDMP, respectively, and the succinimidyl ester of C_6-NBD. C_5-Bodipy-Cer was synthesized from D-*erythro*-sphingosine and Bodipy™-503/512-C_5. C_6-GlcCer was synthesized from 1-β-D-glucosylsphingosine and hexanoic acid. For cell incubations, C_6-(NBD-)sphingolipid/PDMP solutions were made by ethanol injection in serum-free culture medium (0.5% [vol/vol] final ethanol concentration; see also Kok et al., 1992).

Lipid Extraction and Analysis

Approximately 10^7 HT29 G+ or NRK cells were incubated with 10 μM C_6-NBD-Cer for 60 min at 37°C. After these incubations, the cells together with the incubation medium were subjected to lipid extraction by the procedure of Bligh and Dyer (1959). C_6-NBD-sphingolipids were separated by high performance thin layer chromatography (HPTLC) using CH_3Cl/CH_3OH/20% (wt/vol) NH_4OH (14:6:1, vol/vol/vol) as the running solvent system. Individual C_6-NBD-sphingolipid species (Cer, GlcCer, and SM) were scraped from the HPTLC plates and eluted from the silica with 1% (vol/vol) Triton X-100 by vigorous shaking at 37°C. Individual C_6-NBD-sphingolipid species were quantified by measuring the NBD fluorescence in a fluorimeter at an excitation wavelength of 465 nm and an emission wavelength of 530 nm.

Measurement of C_6-NBD-PDMP Uptake, Efflux, and Accessibility to Sodium Dithionite

Approximately 10^7 HT29 G+ cells were washed with Hanks' solution and incubated with 10 μM C_6-NBD-PDMP for 30 min at 37°C. The incubation buffer was aspirated and replaced by fresh Hanks' solution, followed by incubations at 37°C for various time intervals. At each time point, both the cell fraction and the incubation medium were subjected to lipid extraction (see above). The amount of C_6-NBD-PDMP in each fraction was measured in a fluorimeter as described above. In all experiments, mock-treated cells were subjected to lipid extraction and fluorescence measurement. These background values were subtracted from the values of cells, which had been incubated with C_6-NBD-PDMP.

For sodium dithionite quenching studies, the initial 37°C incubation with 10 μM C_6-NBD-PDMP was followed by a 30-min incubation in Hanks' solution containing 30 mM $Na_2S_2O_4$ (diluted from a stock solution of 1 M $Na_2S_2O_4$ in 1 M Tris, pH 10; c.f. McIntyre and Sleight, 1991). Control cells were incubated in Hanks' solution without sodium dithionite. To study the effect of sodium dithionite on C_6-NBD-Cer, cells were incubated with 10 μM C_6-NBD-Cer for 30 min at 37°C, followed by a "back-exchange" at 2°C. To this end, cells were incubated with 5% (wt/vol) BSA in Hanks' solution for 30 min at 2°C, followed by extensive washing. Thereafter, cells were incubated in Hanks' solution with or without 30 mM $Na_2S_2O_4$ for 30 min at 37°C, followed by a back-exchange at 2°C. Back-exchanges were performed to ensure that plasma membrane pools of C_6-NBD-lipid did not contribute to the measured values in control cells. These pools consist of C_6-NBD-Cer, which was initially inserted in

the plasma membrane, and/or C_6-NBD-sphingolipid products, which were synthesized in the Golgi apparatus and transported to the plasma membrane. In cells subjected to dithionite, quenching of this pool of C_6-NBD-lipid will occur. In contrast to the experiments with C_6-NBD-Cer, in the case of C_6-NBD-PDMP, similar results were obtained, regardless of whether the back-exchange had been carried out.

In all experiments, total lipid phosphorus was determined in each fraction after perchloric acid destruction according to Böttcher et al. (1961). In addition, in cell fractions the number of cells was counted. All C_6-NBD-PDMP/Cer determinations were normalized to total lipid phosphorus.

Fluorescence Microscopy

Cells were grown on glass coverslips contained in 35-mm-diam Petri dishes. Experiments were carried out 72 h after passage. Before experiments, the cells were cooled (30 min) and washed several times with ice-cold Hanks' solution. Cells were incubated with C_6-NBD-Cer (5 μM) in Hanks' solution at 2°C for 1 h, followed by a wash with Hanks' buffer. Subsequently, the cells were subjected to 30-min incubations with Hanks' solution, containing 5 μg/ml BFA, 100 μM (lyso-)PDMP, or both, at 37°C. Occasionally, either C_6-Cer or C_6-GlcCer (both 100 μM), or one of the MDR inhibitors was included. Also during these incubations, C_6-NBD-Cer (2 μM) was present. Finally, a back-exchange was performed by incubating the cells with 5% BSA in cold (2°C) Hanks' solution for 30 min, followed by extensive washing. In the case of intracellular PDMP localization, cells were incubated with C_6-NBD-PDMP (100 μM) in Hanks' solution for 30 min at 37°C. The effect on Golgi morphology was in this case monitored by using C_5-Bodipy-Cer. For this purpose, cells were preincubated with 5 μM C_5-Bodipy-Cer for 60 min at 37°C to ensure that high enough concentrations of Bodipy-sphingolipids at the Golgi apparatus were reached for a spectral shift in fluorescence to occur (Pagano et al., 1991). For dithionite quenching, cells were incubated with Hanks' solution containing 30 mM $Na_2S_2O_4$ (diluted from a stock solution of 1M $Na_2S_2O_4$ in 1 M Tris, pH 10; c.f. McIntyre and Sleight, 1991) for 30 min at 37°C, allowing fluid-phase uptake of this NBD quencher in endocytic compartments to occur. Hence, this procedure will result in loading of the endo/lysosomal system with the NBD quencher (Kok et al., 1995).

For immunocytochemical studies, following various incubation schemes with BFA and/or PDMP, cells were fixed in −20°C methanol for 30 min. Thereafter, cells were washed four times with PBS, followed by a 30-min incubation with PBS/1% (wt/vol) BSA. Fixed cells were incubated overnight at 4°C with the primary antibody diluted in PBS/1% (wt/vol) BSA (anti-ManII: diluted 1:4,000 for NRK cells and 1:80 for HT29 G+ cells; 18B11: diluted 1:100), followed by two washes with PBS/1% (wt/vol) BSA. Thereafter, fixed cells were incubated for 60 min at room temperature with the secondary antibody TRITC anti–rabbit IgG $F(ab')_2$ fragment (dilution 1:30), followed by two washes with PBS/1% (wt/vol) BSA. In case of double immunofluorescence staining, the cells were incubated with two primary antibodies (anti-ManII and anti–β-COP: diluted 1:20) overnight and subsequently with FITC anti–rabbit IgG $F(ab')_2$ fragment + TRITC anti–mouse IgG $F(ab')_2$ fragment (dilutions 1:30) for 60 min. Finally, fixed cells were mounted and examined by fluorescence microscopy. Fluorescence microscopy was performed with an Olympus (Melville, NY) AX-70 research microscope, equipped with a PM20 photomicrography system. Photomicrographs were taken with 10-s (NBD fluorescence) or 1-min (FITC/TRITC fluorescence) exposure times using Ilford (Cheshire, UK) HP5 film that was processed at 1,600 ASA. All images from HT29 cells were taken with a confocal scanning laser microscope (True Confocal Scanner 4D; Leica, Heidelberg, Germany) equipped with an argon-krypton laser and coupled to a Leitz DM IRB inverted microscope (Leica). Images were taken at 488 nm for NBD fluorescence and 562 nm for Bodipy/TRITC fluorescence.

Calcium Measurements

Intracellular calcium concentrations were measured as described previously (Sipma et al., 1995; Filipeanu et al., 1997). After trypsinization, the cells were suspended in Hanks' solution at a concentration of 10^7 cells/ml. The cells were incubated with 2 μM indo-1/AM at room temperature for 30 min in the dark. The cells were collected by centrifugation and washed twice with Hanks' solution before fluorescence measurements. Intracellular indo-1 fluorescence was measured in a spectrophotometer (model Aminco®-Bowman; Spectronic Instruments, Inc., Rochester, NY), using 10^6 cells/ml for each measurement. Measurement was performed at 23°C to prevent dye compartmentalization and leakage. The excitation wavelength was 349 nm, and emission at 410 and 490 nm were acquired with a frequency of 1 Hz. Drugs were added with a Hamilton syringe to a magnetically stirred cell suspension in a volume <1% of the total cell suspension volume (3 ml). Actual $[Ca^{2+}]_i$ values were calculated by a classical equation (Grynkiewicz et al., 1985) using R_{max} and R_{min} values obtained at the end of each experiment using 60 mg/ml saponin and 20 mM EGTA, pH 8.0, respectively. Autofluorescence of the cells, i.e., the signal remaining after 10 mM $MnCl_2$ addition, was subtracted before calculation. Calcium-free medium is defined as Hanks' buffer to which 1.5 mM EGTA is added (final $[Ca^{2+}]_i < 1$ μM).

Results

PDMP Inhibits BFA-induced Retrograde Golgi to ER Lipid Flow in HT29 Cells

As shown in Fig. 1 *B*, incubation of HT29 G+ cells with BFA resulted in loss of discrete Golgi structures that had been labeled with C_6-NBD-Cer (compare to control cells in Fig. 1 *A*). However, when BFA incubation had been preceded by PDMP treatment (Fig. 1 *E*), discrete Golgi structures were still observed. Apparently, PDMP blocked the BFA-induced retrograde C_6-NBD-lipid flow from Golgi to ER. The observed effects were critically dependent on the order of addition of both drugs. Thus, when BFA was allowed to act before PDMP was added to the cells (Fig. 1 *F*), discrete Golgi structures were no longer detectable, i.e., all Golgi membranes had already merged with the ER compartment by BFA-induced retrograde flow. In the case when both drugs were added simultaneously (Fig. 1 *D*), Golgi compartments did not disappear.

Inhibition of BFA-induced Retrograde Transport by PDMP Is Not Restricted to Lipids; PDMP Blocks Membrane Flow

To investigate whether the effect of PDMP was specific for (C_6-NBD-)lipid flow or was due to a general block of membrane flow, the following experiments were performed. Cells were treated with BFA and/or PDMP, as in Fig. 1, *A–F*, but instead of monitoring the fate of C_6-NBD-Cer in living cells, the localization of a Golgi resident protein was assessed after fixation of the cells. As shown in Fig. 1, *G–N*, the fate of a *cis/medial*-Golgi resident protein, ManII, was very similar to that observed for C_6-NBD-Cer in living cells. Indeed, BFA treatment (Fig. 1 *H*) caused a loss of discrete Golgi structures, while PDMP resulted in maintenance of the Golgi compartment, provided that it had been administered before (Fig. 1 *M*) or together with (Fig. 1 *L*) BFA. In conclusion, not only is BFA-induced retrograde lipid flow inhibited by PDMP, but the entire membrane flow is blocked.

Inhibition of BFA-induced Retrograde Membrane Flow by PDMP Is Not Restricted to HT29 Cells

The effect of PDMP on BFA-induced retrograde Golgi to ER membrane flow was not a feature that occurred only in the human HT29 G+ colon tumor cell line. In an entirely different cell type, the NRK fibroblast, PDMP affected BFA-induced retrograde membrane flow as well, as indicated by either C_6-NBD-Cer labeling (Fig. 2, *A–F*) or ManII staining (Fig. 2, *G–N*). Note that when PDMP was administered simultaneously with BFA in NRK cells (Fig. 2, *D* and *L*), the Golgi complex appeared swollen, while

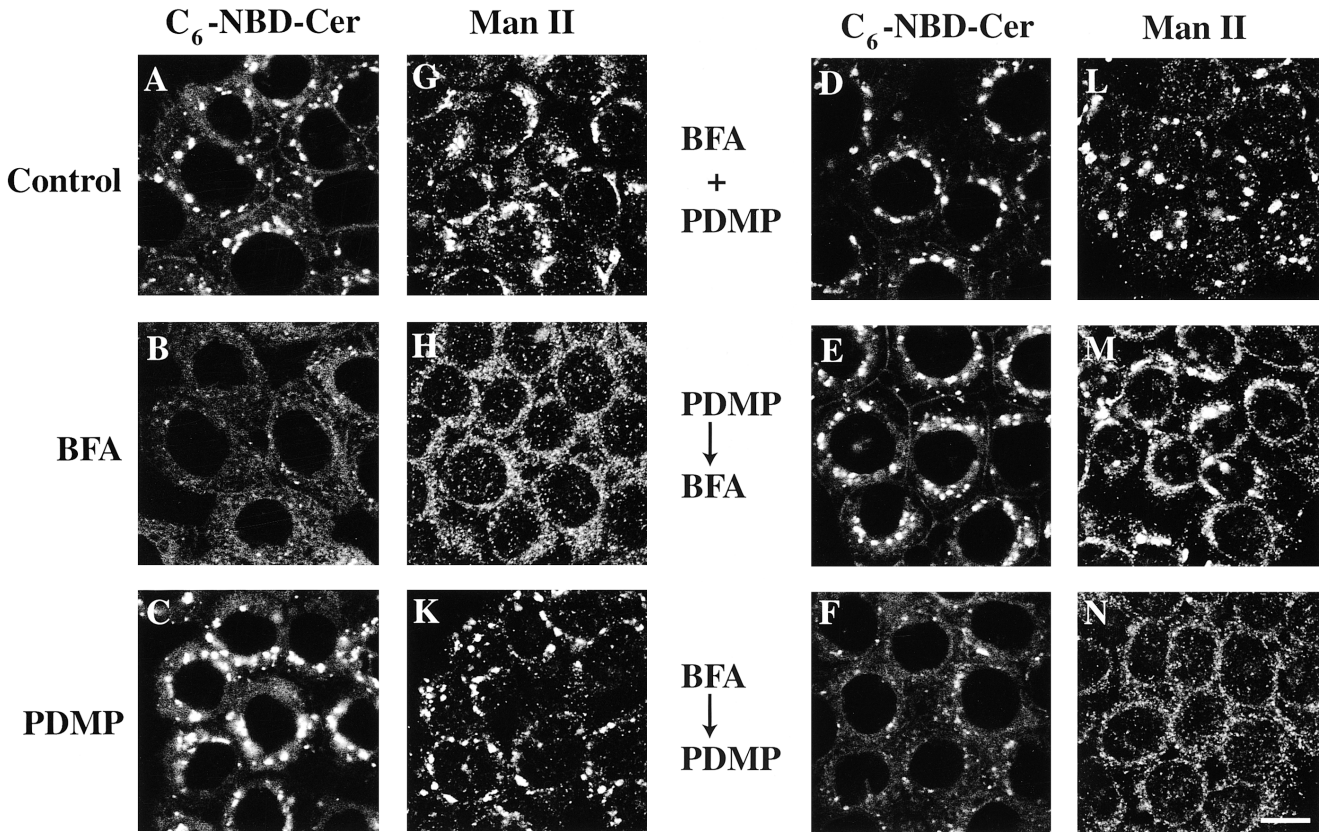

Figure 1. PDMP inhibits BFA-induced retrograde membrane flow from Golgi to ER in HT29 cells. HT29 G+ cells, grown on coverslips, were incubated for 30 min at 37°C in Hanks' solution (control; *A* and *G*) or in Hanks' containing 5 μg/ml BFA (*B* and *H*), 100 μM PDMP (*C* and *K*), or both BFA and PDMP (*D* and *L*). In *E* and *M*, the 30-min incubation with BFA + PDMP was preceded by a 30-min incubation with PDMP, while in *F* and *N*, it was preceded by a 30-min incubation with BFA. One series (*A–F*) shows living cells (pre-)incubated with C_6-NBD-Cer (see Materials and Methods). In the other series (*G–N*), cells were fixed after the incubations with inhibitors and processed for immunocytochemical staining using an antibody against ManII. Images were taken with confocal scanning laser microscopy. Bar, 10 μm.

C_6-NBD-lipid staining suggested the presence of tubules (Fig. 2 *D*). These structural changes were not observed when PDMP was allowed to exert its effect before BFA addition. It thus appeared that PDMP interfered with the ongoing redistribution of membranes into the ER, just after the onset of this process induced by BFA. A *trans*-Golgi resident protein, $GMP_{t\text{-}1}$ (Alcade et al., 1992, 1994), was also affected by PDMP treatment (Fig. 2, *P–V*), although in this case some residual Golgi structure was observed in BFA-treated cells.

Characteristics of the PDMP block of BFA-induced Retrograde Membrane Flow

Although most experiments were performed at the time scale of 1 h, the effect of PDMP on BFA-induced retrograde Golgi to ER membrane flow was also observed after extended incubation time intervals. BFA + PDMP treatment during 3 h did not result in disappearance of discrete Golgi structures (Fig. 3 *A*; c.f. Fig. 2 *L*). When PDMP was removed from the medium, its inhibiting effect on BFA-induced retrograde membrane flow turned out to be reversible. After an initial incubation with PDMP + BFA for 30 min (Fig. 3 *B*), a subsequent incubation with BFA alone resulted in a gradual loss of discrete Golgi structures (Fig. 3, *C* and *D*). Note that only 3 h after the withdrawal of PDMP, the effect of BFA was completed.

The effect of PDMP on BFA-induced retrograde membrane flow was concentration dependent. This was observed when cells were incubated with PDMP at various concentrations, ranging from 10 to 100 μM (in steps of 10 μM), followed by incubation with both PDMP (at the respective concentrations) and BFA. In HT29 cells, the inhibition of BFA-induced retrograde membrane flow, as monitored by C_6-NBD-Cer staining, became apparent at a PDMP concentration of 50 μM, although not all cells were affected at this concentration. NRK cells appeared to be slightly less sensitive, as inhibition became apparent at 80 μM. Furthermore, the inhibitory effect of PDMP required the intact molecule because lyso-PDMP, which lacks the fatty-acyl moiety, was not able to block BFA-induced retrograde membrane flow in both HT29 G+ and NRK cells (Fig. 4).

PDMP Does Not Impair Coatomer Detachment Induced by BFA

BFA-induced dissociation of coatomer from membranes

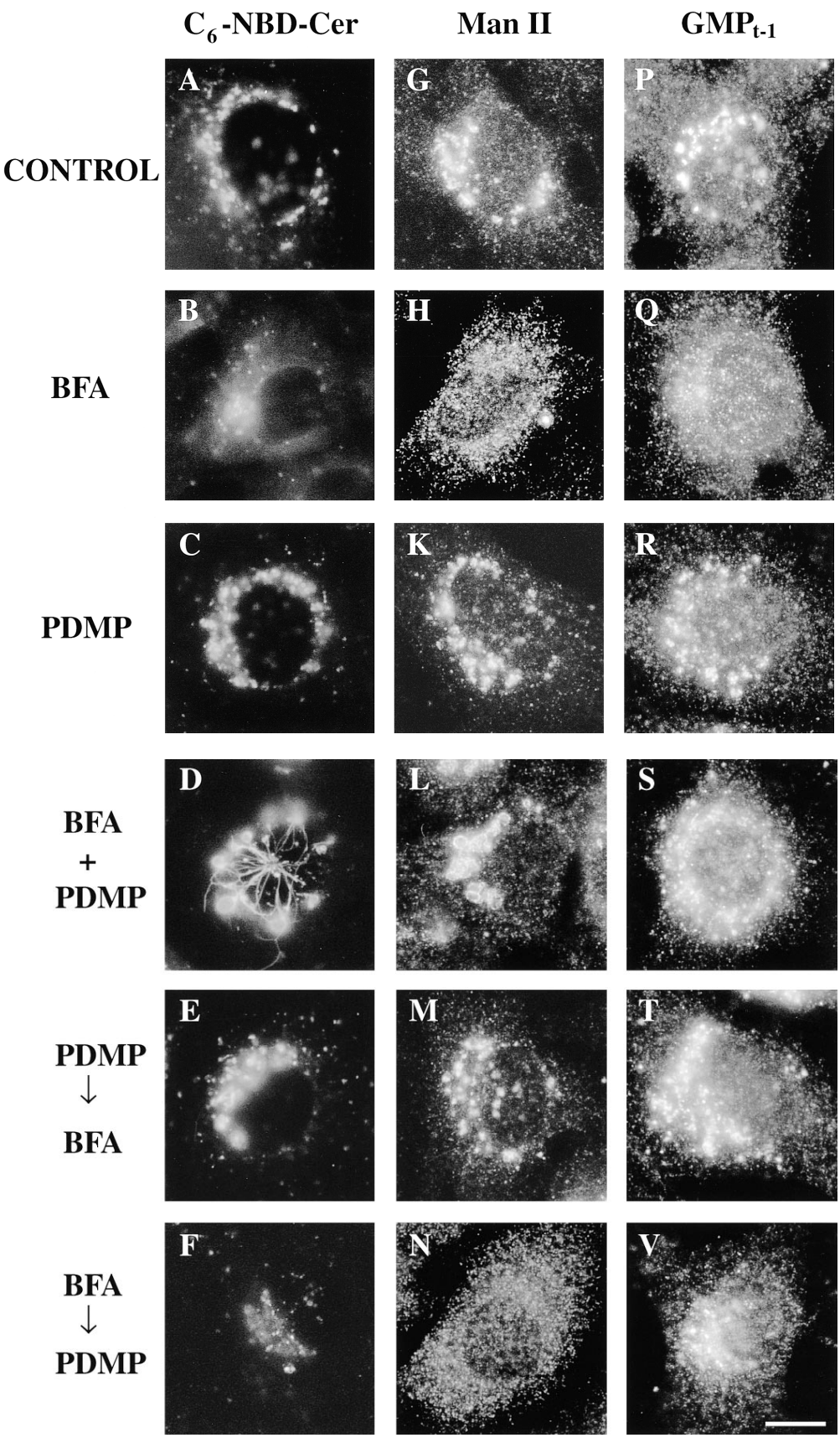

Figure 2. PDMP inhibits BFA-induced retrograde membrane flow from Golgi to ER in NRK cells. NRK fibroblasts, grown on coverslips, were incubated for 30 min at 37°C in Hanks' solution (control; *A*, *G*, and *P*) or in Hanks' containing 5 μg/ml BFA (*B*, *H*, and *Q*), 100 μM PDMP (*C*, *K*, and *R*), or both BFA and PDMP (*D*, *L*, and *S*). In *E*, *M*, and *T*, the 30-min incubation with BFA + PDMP was preceded by a 30-min incubation with PDMP, while in *F*, *N*, and *V*, it was preceded by a 30-min incubation with BFA. One series (*A–F*) shows living cells (pre-) incubated with C_6-NBD-Cer (see Materials and Methods). In the other two series, cells were fixed after the incubations with inhibitors and processed for immunocytochemical staining using antibodies against ManII (*G–N*) or GMP_{t-1} (*P–V*). Bar, 10 μm.

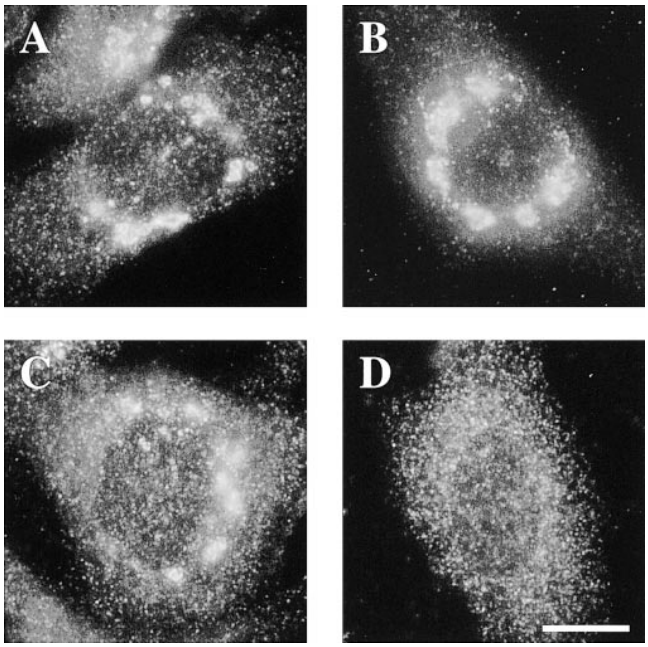

Figure 3. Inhibition by PDMP of BFA-induced membrane flow is reversible. NRK fibroblasts, grown on coverslips, were incubated for 3 h at 37°C in Hanks' solution containing 100 μM PDMP + 5 μg/ml BFA (*A*). Alternatively, cells were in this solution for 30 min (*B*), followed by three Hanks' washes and subsequent incubation with BFA alone for 1 (*C*) or 3 h (*D*). After these incubations, cells were fixed and processed for immunocytochemical staining using an antibody against ManII. Note that discrete, swollen Golgi structures gradually disappear during the BFA chase incubation. Bar, 10 μm.

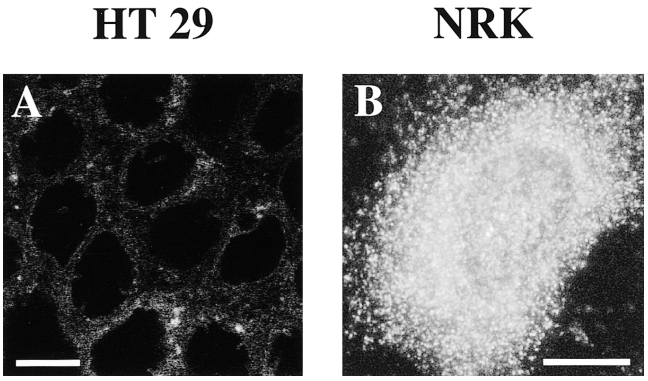

Figure 4. Lyso-PDMP does not inhibit BFA-induced retrograde membrane flow. HT29 G+ (*A*) or NRK (*B*) cells, grown on coverslips, were incubated for 30 min at 37°C in Hanks' solution containing 100 μM lyso-(D,L-*threo*-)PDMP, followed by another 30-min incubation with lyso-PDMP + 5 μg/ml BFA. In *A*, living cells were incubated with C_6-NBD-Cer as a Golgi stain, and the image was taken with confocal scanning laser microscopy. In *B*, after the incubations, cells were fixed and processed for immunocytochemical staining using an antibody against ManII. The latter image was taken with conventional fluorescence microscopy. Bars, 10 μm.

precedes and is required for redistribution of Golgi membranes into the ER compartment (Scheel et al., 1997). When the distribution of the coatomer protein subunit β-COP (Aridor and Balch, 1996; Bednarek et al., 1996) was analyzed in PDMP- and BFA-treated NRK cells, it turned out that its release from the Golgi complex, as induced by BFA, was not prevented by PDMP (Fig. 5). Regardless of whether BFA-treated cells were initially (Fig. 5 *L*) or simultaneously (Fig. 5 *H*) incubated with PDMP, β-COP was released, indistinguishably from its release in cells treated with BFA alone (Fig. 5 *D*). Note that release of β-COP occurred under conditions where the Golgi complex did not disappear (Fig. 5, *G* and *K*), while PDMP by itself did not affect the distribution of β-COP (Fig. 5 *F*, compare with *B* and *D*).

PDMP Effect on BFA-induced Retrograde Golgi to ER Membrane Flow Is Not Correlated to Inhibition of SM Biosynthesis

A correlation between anterograde membrane transport in the biosynthesis pathway and SM biosynthesis has been suggested by Rosenwald et al. (1992) for CHO cells. Since PDMP is known to affect sphingolipid metabolism in other cell types as well (Radin et al., 1993), our results regarding inhibition of BFA-induced retrograde membrane transport might be explained similarly. However, while GlcCer biosynthesis is very sensitive to PDMP in all cell types tested (Table I; c.f. Rosenwald et al., 1992), the effect of PDMP on SM biosynthesis is less drastic and, furthermore, cell type dependent. In CHO cells, SM biosynthesis is inhibited at PDMP concentrations above 40 μM (Rosenwald et al., 1992), coinciding with concentrations that impair anterograde VSV-G protein transport. In the present work, using NRK cells, inhibition of SM biosynthesis occurred with 100 μM PDMP (Table I). Yet in HT29 G+ cells, no inhibition of SM biosynthesis was found (Table I). In conclusion, PDMP had different effects on C_6-NBD-SM biosynthesis in NRK and HT29 cells, while in both cell types BFA-induced retrograde membrane flow was inhibited. Therefore, these results argue against a correlation between inhibition of BFA-induced retrograde membrane flow and the biosynthesis of SM.

PDMP Inhibition of BFA-induced Retrograde Golgi to ER Membrane Flow Is Not Mimicked by C_6-Cer or Rescued by C_6-GlcCer

Apart from an effect on the levels of GlcCer and SM, PDMP treatment could result in an increase in Cer. The latter has been correlated with an inhibition of protein trafficking through the secretory pathway (Rosenwald and Pagano, 1993). To establish whether the block in BFA-induced retrograde membrane flow from Golgi to ER could be attributed to an increase in Cer or a decrease in GlcCer, the following experiments were performed. C_6-NBD-Cer–labeled HT29 G+ cells were initially incubated with either C_6-Cer or a combination of PDMP and C_6-GlcCer. This was done to mimic a possible increase in Cer by PDMP or to compensate for the loss of GlcCer due to treatment with the drug, respectively. If the action of PDMP proceeded through changes in sphingolipid levels, one could expect that C_6-Cer mimicked the action of PDMP or that the effect of the drug was counteracted by supplying the cells with GlcCer. As shown in Fig. 6, this was not the case, even at the high concentrations (100 μM)

of (nonfluorescent) short-chain sphingolipids that were used. Incubation with 100 μM C_6-Cer did not result in preservation of discrete Golgi structures (Fig. 6, *A* and *C*) during subsequent incubation with BFA, while the addition of C_6-GlcCer did not result in loss of discrete Golgi structures in PDMP-treated cells (Fig. 6, *B* and *D*). In conclusion, inhibition of BFA-induced retrograde membrane flow does not appear to be correlated to changes in either GlcCer or Cer levels.

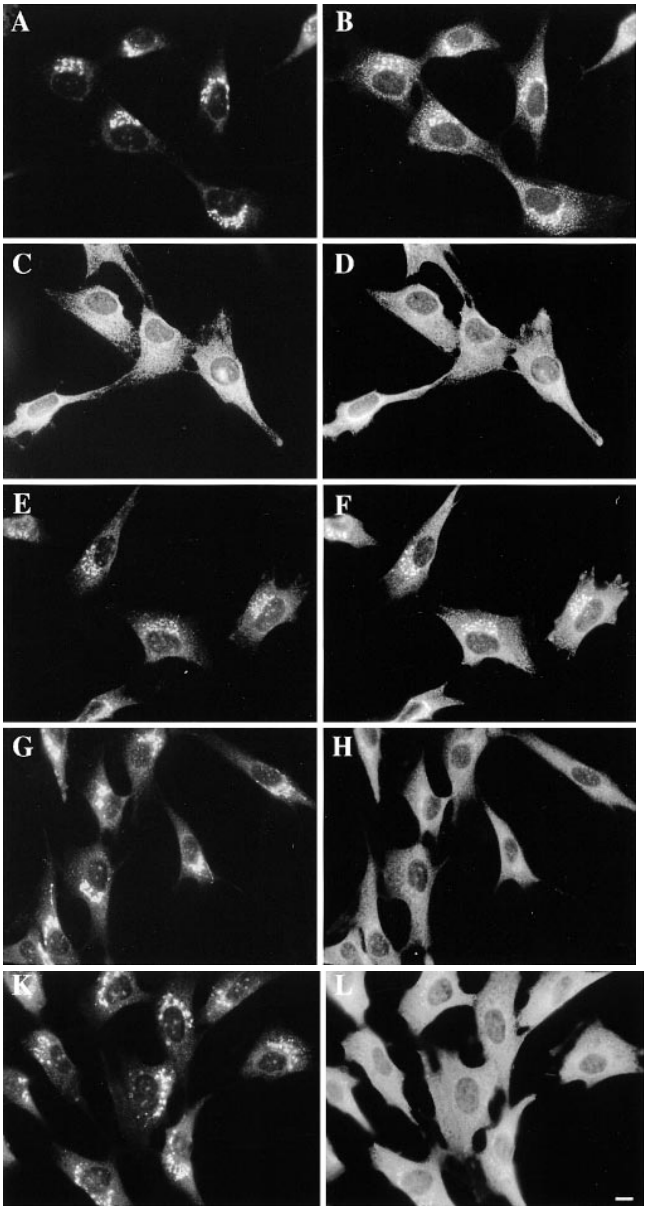

Figure 5. PDMP does not interfere with BFA-induced release of β-COP from Golgi. NRK fibroblasts, grown on coverslips, were incubated for 30 min at 37°C in Hanks' solution (control; *A* and *B*) or in Hanks' containing 5 μg/ml BFA (*C* and *D*), 100 μM PDMP (*E* and *F*), or both BFA and PDMP (*G* and *H*). In *K* and *L*, the 30-min incubation with BFA + PDMP was preceded by a 30-min incubation with PDMP. After the incubations, cells were fixed and processed for immunocytochemical double-staining using antibodies against ManII (*A–K*) and β-COP (*B–L*) in the same cells. Polyclonal anti-ManII antibodies were visualized with FITC anti–rabbit IgG F(ab′)$_2$ fragments and monoclonal β-COP antibodies with TRITC anti–mouse IgG F(ab′)$_2$ fragments. Note that PDMP does not interfere with BFA-induced β-COP release (*H* and *L*) but does not cause release by itself (*F*). Bar, 10 μm.

Table I. Effect of PDMP on C_6-NBD-Sphingolipid Biosynthesis

	C_6-NBD-GlcCer	C_6-NBD-SM
	(percentage of total C_6-NBD-lipid)	(percentage of total C_6-NBD-lipid)
HT29 control	2.5 ± 0.26	3.5 ± 0.38
HT29 PDMP	n.d.*	4.1 ± 0.29
NRK control	1.9 ± 0.15	10.3 ±1.3
NRK PDMP	n.d.*	4.8* ± 0.35

Approximately 10^7 HT29 G+ or NRK cells were incubated for 60 min at 37°C with 10 μM C_6-NBD-Cer in Hanks' solution (control) or the same containing 100 μM D,L-*threo*-PDMP. After these incubations, total C_6-NBD-lipid (cell-associated + in the incubation solution) was extracted, separated by HPTLC, and quantified (see Materials and Methods). The biosynthesis of C_6-NBD-GlcCer and C_6-NBD-SM is expressed as the percentage of total C_6-NBD-lipid. Values are the means (±SD) of triplicate measurements. Asterisks indicate values that are significantly different from control according to student's *t* test ($P < 0.05$).
n.d., not detectable.

C_6-NBD-PDMP Is Localized in Endo/lysosomal Compartments, While It Affects Membrane Flow in the ER/Golgi System

To further investigate the mechanism of action of PDMP

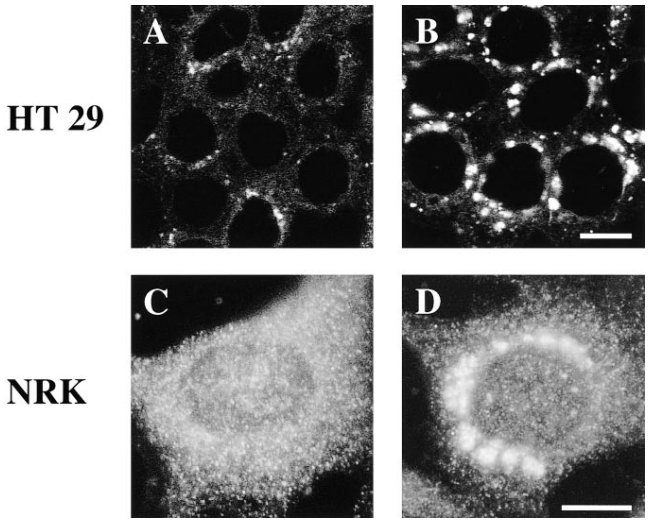

Figure 6. Inhibition of BFA-induced retrograde membrane flow is not mimicked by C_6-Cer or counteracted by C_6-GlcCer. HT29 G+ (*A*) or NRK (*C*) cells, grown on coverslips, were incubated for 30 min at 37°C in Hanks' solution containing 100 μM C_6-Cer, followed by a 30-min incubation with 5 μg/ml BFA + C_6-Cer. In *B* (HT29) and *D* (NRK), cells were incubated during 30 min at 37°C with 100 μM PDMP + 100 μM C_6-GlcCer, followed by a 30-min incubation with BFA + PDMP + C_6-GlcCer. In *A* and *B*, living HT29 G+ cells were incubated with C_6-NBD-Cer as a Golgi stain, and images were taken with confocal scanning laser microscopy. In *C* and *D*, NRK cells are shown, which were fixed after the incubation protocol and processed for immunocytochemical staining using an antibody against ManII. The latter images were taken with conventional fluorescence microscopy (*C* and *D*). Bars, 10 μm.

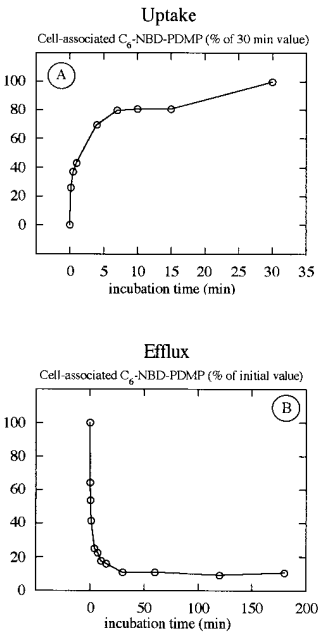

Figure 7. Uptake and efflux of C_6-NBD-PDMP by HT29 cells. (*A*) Approximately 10^7 HT29 G+ cells were incubated with Hanks' solution containing 10 μM C_6-NBD-PDMP for various time intervals at 37°C. The incubation solution was aspirated, and the cells were washed with Hanks' solution. Thereafter, the cells were subjected to lipid extraction, followed by TLC and scraping of C_6-NBD-PDMP spot. The fluorescent PDMP was eluted from the silica by shaking in 1% Triton X-100 and measured in a fluorimeter. Values are expressed as the percentage of uptake at 30 min and represent the average of duplicate measurements. (*B*) Approximately 10^7 HT29 G+ cells were incubated with Hanks' solution containing 10 μM C_6-NBD-PDMP for 30 min at 37°C, followed by a chase in Hanks' solution during various time intervals. Finally, the incubation solutions and the cells were separated and subjected to lipid extraction, followed by fluorescence measurement as described. Cell-associated C_6-NBD-PDMP after 30 min uptake and after various chase incubations is expressed as the percentage of total fluorescence (i.e., cell-associated + excreted). Values are the means of duplicate measurements.

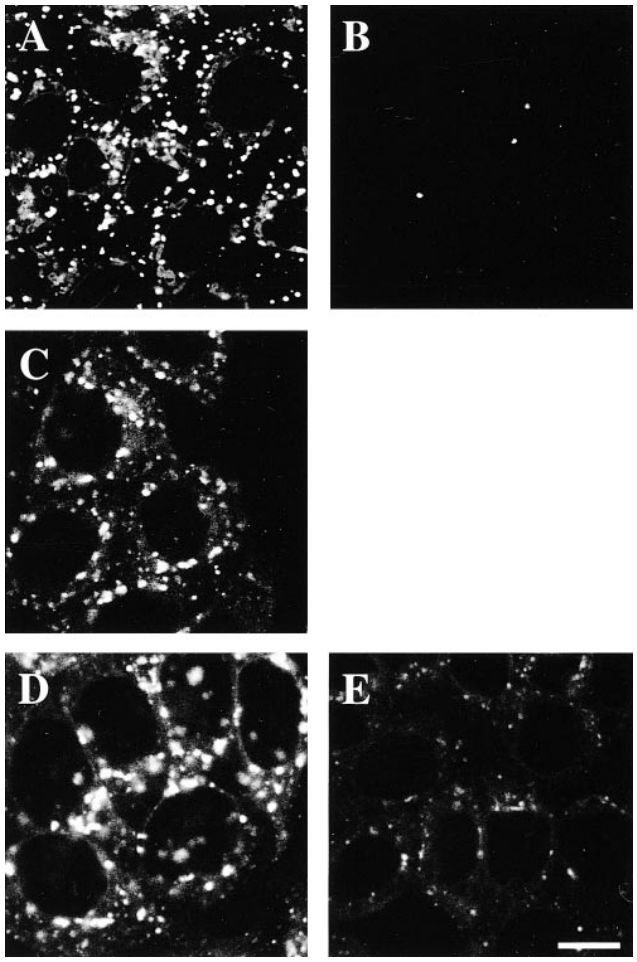

Figure 8. Intracellular localization and effect of C_6-NBD-PDMP. HT29 G+ cells, grown on coverslips, were incubated for 30 min at 37°C in Hanks' solution containing 100 μM C_6-NBD-PDMP (*A*). In *B*, this incubation was followed by a 30-min incubation with Hanks' containing 30 mM $Na_2S_2O_4$. In a parallel experiment, cells were incubated with 5 μM C_6-NBD-Cer for 30 min at 37°C, followed by a 30-min incubation with Hanks' containing 30 mM $Na_2S_2O_4$ (*C*). In all cases, the cells were subjected to a back-exchange procedure at the end of the experiment. In *D* and *E*, HT29 G+ cells were subjected to three subsequent incubations: with 5 μM C_5-Bodipy-Cer for 60 min at 37°C; a 30-min incubation with 100 μM C_6-NBD-PDMP (*D*) or 5 μg/ml BFA (*E*); and a 30-min incubation with 100 μM C_6-NBD-PDMP + 5 μg/ml BFA + 30 mM $Na_2S_2O_4$ (*D* and *E*). Images were taken with confocal scanning laser microscopy. Bar, 10 μm.

on membrane flow, we synthesized a fluorescent analogue of the drug, C_6-NBD-PDMP, enabling the study of uptake, efflux, and intracellular localization of the drug. As shown in Fig. 7 *A*, C_6-NBD-PDMP was rapidly taken up by HT29 G+ cells. Incubation with 10 μM C_6-NBD-PDMP for 30 min at 37°C resulted in uptake of 1.58 pmol C_6-NBD-PDMP/nmol cellular lipid phosphorus ($n = 2$), or 3.74×10^7 molecules/cell. This was 3.8% of the total amount of C_6-NBD-PDMP administered to the cells. Half of this uptake was already achieved after 1.8 min (Fig. 7 *A*). Interestingly, when the C_6-NBD-PDMP–containing incubation solution was removed and the cells were subsequently incubated in fresh Hanks' solution, a rapid efflux of C_6-NBD-PDMP occurred (Fig. 7 *B*). Half of the initial cell-associated pool was released into the incubation solution after only 40 s, while within 30 min 89% was released. The residual intracellular pool remained constant during prolonged incubation up to at least 3 h (Fig. 7 *B*). TLC analysis revealed that C_6-NBD-PDMP was not metabolized to lyso-PDMP and NBD-C_6–fatty acyl chain during these incubations (data not shown).

When HT29 G+ cells were incubated with 100 μM C_6-NBD-PDMP for 30 min at 37°C, a staining pattern was observed (Fig. 8 *A*), which is indicative of a primary localization of the drug in endocytic organelles. This was further examined by loading the cells with sodium dithionite. This NBD fluorescence quencher is taken up into the endocytic pathway by fluid-phase endocytosis and transported to endocytic compartments, including lysosomes. As a result, the fluorescence of all NBD-labeled molecules residing in endocytic compartments will be quenched (Kok et al., 1995). When such an incubation was performed on cells that had previously taken up C_6-NBD-PDMP, intracellular fluorescence was quenched, as judged by confocal scanning laser microscopy (Fig. 8 *B*). Indeed, when the extent of NBD quenching was measured in a parallel experiment with the same incubation protocol (see Materials and Methods), 91.3% (±5.6; $n = 3$) quenching of C_6-NBD-PDMP was found. It should be noted that, given the experimental setup (see Materials and Methods), the pool of C_6-NBD-PDMP, which is quenched under these condi-

tions, is the residual intracellular pool after large scale efflux (see above). When HT29 G+ cells were labeled with C_6-NBD-Cer, followed by uptake of sodium dithionite, Golgi labeling was readily observed (Fig. 8 *C*), indicating that sodium dithionite did not acquire access to the Golgi apparatus. Determination showed that in this case only 16.7% (±6.9; $n = 3$) quenching of NBD fluorescence occurred. In conclusion, although the cell-biological effect of PDMP is evidently associated with Golgi functioning, the drug itself did not reach this organelle since C_6-NBD-PDMP could not be detected in the Golgi apparatus (c.f. Rosenwald and Pagano, 1994).

An important question to be addressed was whether the fluorescent derivative of PDMP inhibited BFA-induced retrograde Golgi to ER membrane flow, similarly to native drug. HT29 G+ cells were incubated with C_6-NBD-PDMP (100 μM), followed by BFA treatment (Fig. 8 *D*, c.f. to Fig. 1 *E*) or pretreated with BFA, followed by incubation with C_6-NBD-PDMP (Fig. 8 *E*, compare to Fig. 1 *F*). To identify the Golgi in this case, the cells were prelabeled with C_5-Bodipy-Cer instead of C_6-NBD-Cer. Concentration of C_5-Bodipy-sphingolipids at the Golgi apparatus results in red fluorescence (Pagano et al., 1991), which can be discriminated from the green NBD fluorescence of the C_6-NBD-PDMP. As shown in Fig. 8, *D* and *E*, C_6-NBD-PDMP was able to prevent BFA-induced Golgi–ER merging, provided that the fluorescent PDMP analogue was added before BFA. Thus, C_6-NBD-PDMP behaved similarly to PDMP, in terms of inhibition of BFA-induced retrograde membrane flow.

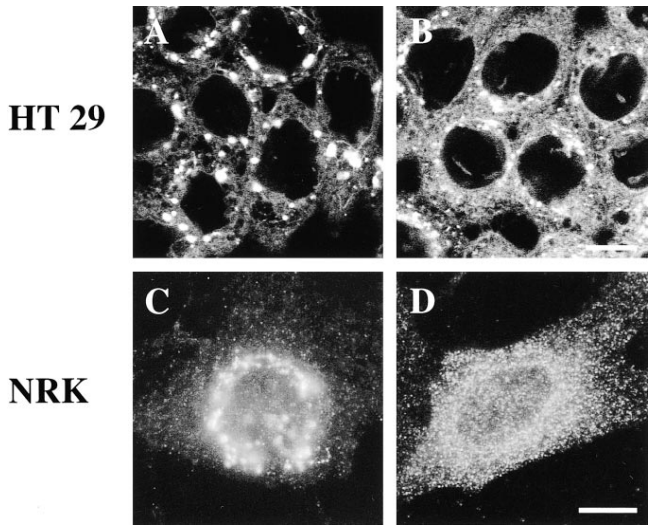

Figure 9. MK571 inhibits BFA-induced retrograde membrane flow. HT29 G+ (*A* and *B*) or NRK (*C* and *D*) cells, grown on coverslips, were incubated for 30 min at 37°C in Hanks' solution containing 50 μM MK571 (*A* and *C*) or 50 μM cyclosporin A (*B* and *D*), followed by another 30-min incubation with the respective drugs + 5 μg/ml BFA. In *A* and *B*, living HT29 G+ cells were incubated with C_6-NBD-Cer as a Golgi stain, and the images were taken with confocal scanning laser microscopy. In *C* and *D*, after the incubations, NRK cells were fixed and processed for immunocytochemical staining using an antibody against ManII. The latter images were taken with conventional fluorescence microscopy. Bars, 10 μm.

The PDMP Effect on BFA-induced Retrograde Membrane Flow in the ER/Golgi System Is Mimicked by MK571

Recently, a correlation was established between the MDR status of cells and the accumulation of glucosylceramides (Lavie et al., 1996). Furthermore, agents that reverse multidrug resistance were shown to inhibit GlcCer synthase, the target of PDMP (Lavie et al., 1997). In view of this similarity in target, we examined whether such MDR-reversing agents could also inhibit BFA-induced retrograde membrane transport. When HT29 G+ or NRK cells were incubated with 50 μM MK571, a specific inhibitor of multidrug resistance protein (MRP) function (Gekeler et al., 1995), followed by incubation with BFA, discrete Golgi structures were observed (Fig. 9, *A* and *C*). Thus, similar to PDMP, this MRP-specific MDR-reversing agent was able to block BFA-induced retrograde membrane flow from the Golgi to the ER. MK571 also caused an inhibition of GlcCer biosynthesis from C_6-NBD-Cer, be it much less efficient than PDMP. In comparison, in HT29 G+ cells 100 μM PDMP inhibited C_6-NBD-GlcCer biosynthesis 34.7-fold (±12.3; $n = 3$), while 50 μM MK571 caused an inhibition of only twofold (±0.4; $n = 3$). MDR-reversing agents acting primarily on P-glycoprotein (P-gp), such as cyclosporin A and PSC833 (Friche et al., 1991; Watanabe et al., 1995), had no effect on C_6-NBD-GlcCer biosynthesis (data not shown). In NRK cells, cyclosporin A and PSC833 did not affect BFA-induced retrograde membrane flow from Golgi to ER (Fig. 9 *D*). In HT29 cells, both P-gp drugs showed some effect, although not as prominent as MK571 (Fig. 9 *B*). Interestingly, when C_6-NBD-PDMP uptake was measured (as shown above) in HT29 G+ cells, its cellular accumulation during a 10-min incubation was increased to 140% ($n = 2$) in the presence of MK571, while cyclosporin A and PSC833 did not modulate its accumulation. The absence of effects of P-gp antagonists is compatible with results from Rosenwald and Pagano (1994), showing that in CHO cells that were selected for increased resistance to PDMP toxicity, this resistance was not mediated by P-gp.

PDMP Modulates Calcium Homeostasis in HT29 Cells in at Least Three Different Ways

To explore the molecular mechanism behind the inhibiting effect of PDMP on BFA-induced retrograde membrane flow, we measured the intracellular calcium concentration in HT29 cells and its potential modulation by PDMP. The rationale for such experiments is rooted in the observations made by Ivessa et al. (1995), who reported that BFA-induced retrograde membrane transport from Golgi to ER depends on calcium homeostasis. When HT29 G+ cells were incubated with PDMP, modulation of $[Ca^{2+}]_i$ was indeed observed (Fig. 10 *A*). The average basal $[Ca^{2+}]_i$ was 144 ± 11 nM ($n = 78$). Addition of 100 μM PDMP resulted in a transient increase of 154 ± 24 nM ($n = 8$) above basal $[Ca^{2+}]_i$. The rise in $[Ca^{2+}]_i$ depended on the concentration of PDMP (Fig. 11 *A*), with a modest increase observed at 50 μM (22 ± 12 nM; $n = 7$) and a large enhancement at 150 μM (445 ± 70 nM; $n = 6$). Below 50 μM, responses were not observed, in accordance with the ab-

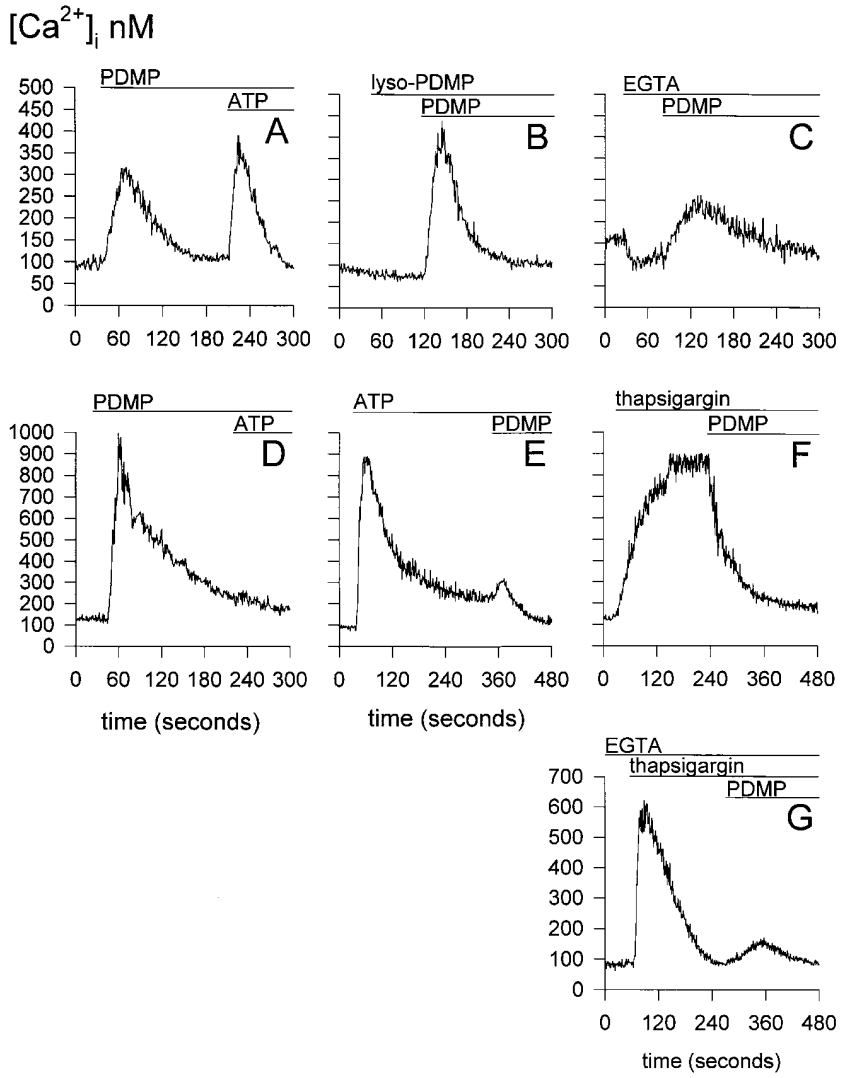

Figure 10. PDMP modulates calcium homeostasis. 10^7 HT29 G+ cells/ml were loaded with 2 μM indo-1/AM (see Materials and Methods), followed by washing and dual-wavelength measurement of fluorescence, using 10^6 cells/ml per measurement. $[Ca^{2+}]_i$ was calculated as described. Single traces are shown, which illustrate the following events: (*A*) A moderate PDMP response (at 100 μM) is followed by an ATP response (at 100 μM). (*B*) Lyso-PDMP (at 100 μM) does not induce a calcium response, while PDMP (at 100 μM) does. (*C*) PDMP (at 100 μM) causes calcium release from an intracellular store(s), as observed in calcium-free medium. (*D*) A high PDMP response (at 150 μM) abolishes the ATP response (at 100 μM). (*E*) A high ATP response (at 100 μM) is followed by a PDMP response (at 100 μM). (*F*) PDMP (at 100 μM) abolishes the secondary calcium influx component of the thapsigargin response (at 1 μM). (*G*) PDMP (at 100 μM) still releases calcium from an intracellular store after thapsigargin-induced ER release (at 1 μM).

sence of effect on BFA-induced retrograde membrane transport at these concentrations. Furthermore, in the very same sample of cells, lyso-PDMP did not elicit any Ca^{2+} response, in contrast to PDMP (Fig. 10 *B*). This observation agrees well with the ineffectiveness of lyso-PDMP regarding modulation of BFA-induced retrograde membrane transport (Fig. 4).

A possible interaction between PDMP and receptor-mediated $[Ca^{2+}]_i$ increases was subsequently studied using extracellular ATP to stimulate P_2 purinoceptors on the plasma membrane of HT29 cells (Nitschke et al., 1993; Zhang and Roomans, 1997). An ATP response could be evoked after an initial PDMP response (Fig. 10 *A*). However, occasionally a very large increase in $[Ca^{2+}]_i$ was observed after addition of 150 μM PDMP. Under these circumstances, the ATP response was completely abolished (Fig. 10 *D*). The extent of inhibition of the ATP response was dependent on the concentration of PDMP (Fig. 11 *B*). Interestingly, with the reversed order of addition, PDMP did still evoke a calcium response even after a very high ATP response (Fig. 10 *E*). Next we analyzed the PDMP response in terms of its components. In calcium-free medium, 100 μM PDMP elicited a calcium response (Fig. 10 *C*), which was very similar to that in calcium-containing medium (155 ± 21 nM; $n = 7$). In fact, at all concentrations of PDMP, the two responses overlapped (Fig. 11 *A*), indicating that the PDMP response can be attributed almost entirely to calcium release from intracellular stores, with a minor contribution of influx from the medium. A large part of the calcium release appeared to be associated with the ER compartment since (*a*) the response is effectively reduced after stimulation of the P_2 purinoceptor by ATP (Fig. 10 *E*), which releases calcium from the ER store (c.f. Salter and Hicks, 1995; Liu et al., 1996), and (*b*) a similar inhibition occurs after addition of thapsigargin (Fig. 10 *G*), a known blocker of the Ca^{2+}-ATPase present on the ER (Lytton et al., 1991), which is followed by a PDMP (100 μM) response of 23 ± 4 nM ($n = 11$) in calcium-free medium. However, the observation that the PDMP response could not be fully blocked by either ATP or thapsigargin strongly suggests that PDMP released calcium from another intracellular pool in addition to the ER. Finally, a third component of the PDMP response was a striking inhibition of calcium influx, as induced by P_2 purinoceptor

stimulation or thapsigargin treatment. As shown in Figs. 10 *E* and 11 *B*, PDMP blocked the sustained $[Ca^{2+}]_i$ increase (influx) component of the ATP response. Furthermore, a drastic inhibition of the influx component of the thapsigargin response occurred, as shown in Figs. 10 *F* and 11 *C*. In contrast to PDMP, none of the other calcium mobilizing compounds ATP or thapsigargin or the Ca^{2+} ionophore ionomycin were able to inhibit BFA-induced retrograde membrane transport from Golgi to ER in our studies in HT29 and NRK cells (Fig. 12).

Discussion

Our results show that PDMP inhibits BFA-induced retrograde membrane flow from the Golgi apparatus to the ER, since the drug impaired the transfer of both lipid and protein components of Golgi membranes to the ER in cells treated with BFA. This reveals a novel action of PDMP, in addition to its known effect on membrane transport through the secretory pathway (Rosenwald et al., 1992). Interestingly, with respect to its mechanism(s) of action, PDMP neither directly counteracted the effect of BFA by interference with the drug's ability to induce release of β-COP from Golgi membranes (c.f. Scheel et al., 1997), nor exerted its effect by modulation of sphingolipid metabolism. Rather, the data strongly support the view that the PDMP-mediated impediment of membrane flow is accomplished via a specific modulation of calcium homeostasis.

Given the well-known effect of PDMP on sphingolipid metabolism, we investigated a potential relation with membrane transport. Rosenwald et al. (1992) have suggested that the inhibition by PDMP of anterograde membrane flow in the Golgi and from Golgi to the plasma membrane is correlated to down-regulation of SM biosynthesis. We do not favor this hypothesis as an explanation for the effect of PDMP on BFA-induced retrograde membrane flow because PDMP did not affect C_6-NBD-SM biosynthesis in HT29 G+ cells while still inhibiting BFA-induced retrograde membrane flow. PDMP is not likely to exert its effect through changes in the levels of GlcCer or Cer either. A rise in the cellular Cer level by exogenous addition of C_6-Cer did not mimic the effect of PDMP on BFA-induced retrograde membrane flow. Exogenous ad-

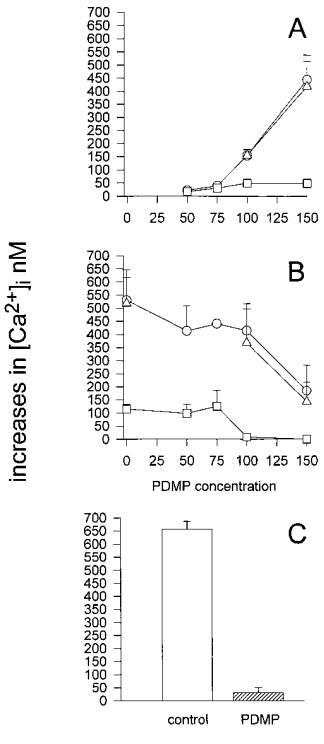

Figure 11. PDMP modulation of $[Ca^{2+}]_i$ and ATP-induced $[Ca^{2+}]_i$ increase is concentration dependent. 10^7 HT29 G+ cells/ml were loaded with 2 μM indo-1/AM (see Materials and Methods), followed by washing and dual-wavelength measurement of fluorescence, using 10^6 cells/ml per measurement. $[Ca^{2+}]_i$ was calculated as described. In *A*, the $[Ca^{2+}]_i$ increase is shown as a function of the PDMP concentration. In *B*, the ATP (100 μM)-induced $[Ca^{2+}]_i$ increase after pretreatment with PDMP is shown as a function of the PDMP concentration. *circles*, total response; *triangles*, response in calcium-free medium; *squares*, calcium influx after $t = 3$ min. *C* shows the effect of 100 μM PDMP on the secondary calcium influx component of the thapsigargin (1 μM) response (c.f. Fig. 10 *F*). Data are the means ± SEM of four to eight independent measurements.

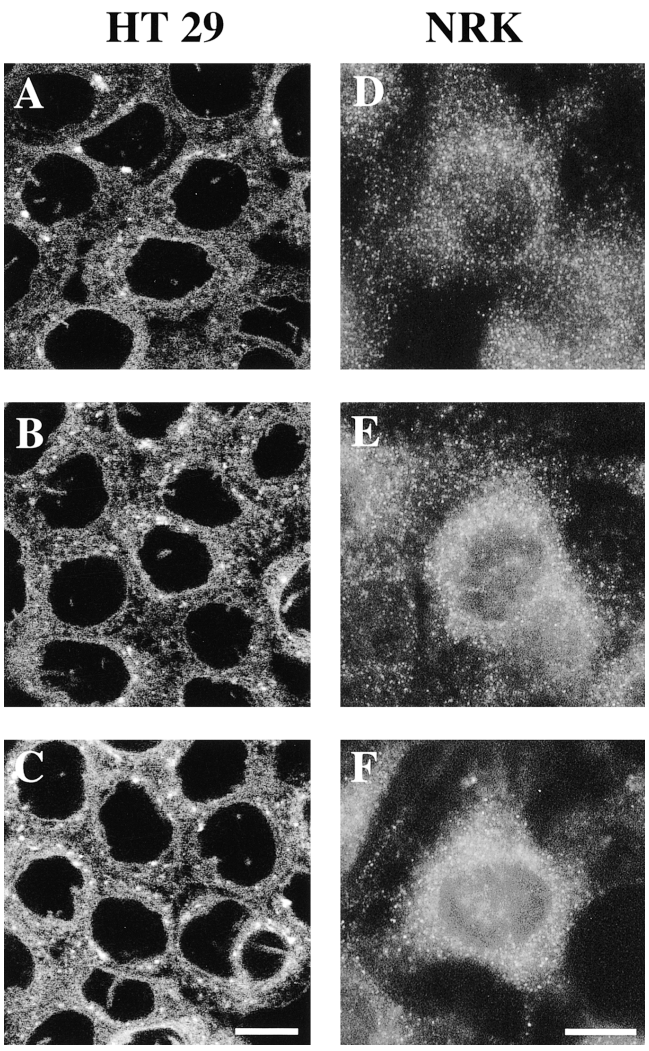

Figure 12. Thapsigargin, ionomycin, and ATP do not inhibit BFA-induced retrograde membrane flow. HT29 G+ (*A–C*) or NRK (*D–F*) cells, grown on coverslips, were incubated for 30 min at 37°C in Hanks' solution containing 1 μM thapsigargin (*A* and *D*), 100 nm (HT29 G+) or 1 μM (NRK) ionomycin (*B* and *E*), or 100 μM ATP (*C* and *F*). This was followed by another 30-min incubation with the respective drugs + 5 μg/ml BFA. In *A–C*, living cells were incubated with C_6-NBD-Cer as a Golgi stain, and the images were taken with confocal scanning laser microscopy. In *D–F*, after the incubations, NRK cells were fixed and processed for immunocytochemical staining using an antibody against ManII. The latter images were taken with conventional fluorescence microscopy. Bars, 10 μm.

dition of C_6-GlcCer, which would compensate for the loss of cellular GlcCer, did not counteract the effect of PDMP. Furthermore, at concentrations below 50 μM, PDMP did not affect BFA-induced retrograde membrane flow but still inhibited GlcCer biosynthesis efficiently (data not shown). In conclusion, the inhibition of membrane flow does not appear to be correlated to fluctuations in sphingolipid levels.

MDR inhibitor studies were prompted by recent observations on the correlation between GlcCer biosynthesis and MDR (Lavie et al., 1996, 1997). Our own observations regarding the fast kinetics of C_6-NBD-PDMP efflux from HT29 cells and its specific modulation by the MRP inhibitor MK571 suggested involvement of MRP pumps in the action of PDMP on membrane transport. Although a specific effect of MK571 (in contrast to the P-gp inhibitors cyclosporin A and PSC833) on BFA-induced retrograde membrane transport was revealed, this experimental approach did not provide insight into the mechanism of action of PDMP. Nevertheless, a correlation with sphingolipid metabolism was again refuted, given the efficient inhibition of BFA-induced retrograde membrane flow by MK571 at a concentration of 50 μM, whereas the effect on GlcCer biosynthesis was marginal compared with PDMP.

More insight into the underlying mechanism of action of PDMP was obtained when modulation of calcium homeostasis by PDMP was investigated, inspired by results from Ivessa et al. (1995), who showed that redistribution of the Golgi complex into the ER is linked to calcium homeostasis in NRK and HeLa cells. An intracellular calcium response was indeed triggered by PDMP, in a similar concentration range as observed for the occurrence of inhibition of BFA-induced retrograde transport (both starting at 50 μM PDMP), while lyso-PDMP served as a negative control regarding both intracellular calcium responses and modulation of BFA-induced retrograde membrane transport. With respect to the low intracellular calcium response at 50 μM PDMP, it should be noted that measurements were performed at room temperature (to avoid compartmentalization of indo-1), which may give rise to an underestimation of the responsiveness at 37°C. Furthermore, as will be pointed out, the absolute size of the calcium response does not appear to be critical. Ivessa et al. (1995) reported that drugs affecting calcium equilibrium, such as thapsigargin and ionomycin, inhibited retrograde membrane transport in the ER/Golgi system in BFA-treated cells. In the present work, we have obtained evidence indicating that a more specific modulation of calcium homeostasis is involved. In our studies in HT29 and NRK cells, ATP, thapsigargin, and ionomycin did not inhibit BFA-induced retrograde transport, suggesting that membrane transport is not associated with calcium release from the ER pool but rather is linked to a specific calcium event. Our detailed analysis of the components of the calcium response to PDMP indicates that in addition to the ER, another PDMP-sensitive calcium pool exists. We have not yet characterized this pool, but it appears to be different from the recently described thapsigargin- and inositol-1,4,5-trisphosphate–insensitive calcium pool (Pizzo et al., 1997), since the latter is ionomycin sensitive. Thus, the size of the calcium response to PDMP, which is mostly determined by the ER release component, is not critical for membrane transport inhibition. Rather, the intracellular localization of the PDMP-sensitive, thapsigargin- and ATP-insensitive calcium pool is likely to be relevant. This pool may function in concert with the shutdown of calcium influx from the medium, as induced by PDMP, constituting the basis of the observed inhibition of BFA-induced membrane transport. A contribution of calcium influx inhibition to the effect of PDMP on membrane transport appears likely given the slow kinetics of reversibility of membrane flow inhibition (Fig. 3). In this respect, it was found that after a single administration of PDMP to cells calcium influx inhibition persisted for at least 2 h (data not shown). The persistent presence of a (C_6-NBD-)PDMP pool of about 13% (Fig. 7 *B*) correlates well with the persistent effect of PDMP on membrane flow and calcium influx inhibition.

Supporting evidence for an indirect mode of action of PDMP, i.e., not related to its interference with sphingolipid metabolism in the Golgi apparatus, includes: (*a*) PDMP acts very quickly, as observed when PDMP, added to cells 3 min after the addition of BFA, still inhibited BFA-induced retrograde membrane transport; only when the preincubation with BFA was extended to 10 min could PDMP not prevent merging of Golgi with ER (data not shown). These results are compatible with modulation of a fast acting Ca^{2+} signaling system within the cell. A prerequisite is its rapid uptake into the cell, which was shown to occur using a fluorescent derivative of PDMP (C_6-NBD-PDMP; Fig. 7 *A*). (*b*) C_6-NBD-PDMP was largely found in endocytic compartments (c.f. Rosenwald and Pagano, 1994), while the fraction residing in the Golgi was too small to be discerned by confocal scanning laser microscopy. It should be noted that the fluorescent analogue of PDMP was as effective as the native drug in causing membrane flow inhibition, ruling out possible artifacts of fluorescent derivatization. Chase experiments revealed that two pools of C_6-NBD-PDMP could be discerned after 30 min incubation with the drug, one of which was rapidly excreted, the other being very stable (Fig. 7 *B*). Also, this stable pool was residing primarily in endocytic compartments since it was almost completely quenched by sodium dithionite. These results show that C_6-NBD-PDMP could not be detected in the Golgi apparatus, and thus indicate the unlikeliness of a direct effect of PDMP on Golgi membrane structure or Golgi membrane proteins involved in transport. A general disrupting effect of PDMP on membrane structure can also be excluded given the transient nature of the intracellular calcium response to PDMP, since a sustained influx would be expected in case of membrane disruption.

All our experiments concerning the effects of PDMP on retrograde membrane flow from Golgi to ER were performed in the context of BFA treatment. Therefore, no conclusions can be drawn with respect to the effect of PDMP on retrograde membrane flow under physiological circumstances, i.e., without BFA, a pathway that functions in the delivery of Golgi- and plasma membrane–localized proteins to the ER (Johannes et al., 1997; Cole et al., 1998). In this respect, PDMP has recently been shown to shift the steady-state distribution of infectious bronchitis virus M protein and ERGIC-53 from the Golgi to the ER in BHK cells under conditions not involving BFA (Maceyka and Machamer, 1997). However, the Golgi

stack markers ManII and giantin were not redistributed, indicating that this effect of PDMP was related to cycling of specific proteins rather than to overall membrane flow. This effect of PDMP was attributed to Cer accumulation, although it was neither completely reversed by metabolic inhibitors of Cer formation nor mimicked by exogenous C_6-Cer addition.

We propose two models for the mechanism by which PDMP and PDMP-induced $[Ca^{2+}]_i$ changes could inhibit BFA-induced retrograde membrane flow. (*a*) PDMP acts independently of BFA in a process (e.g., the actual fusion process) involved in the merging of ER and Golgi membranes during the direct, vesicle budding-uncoupled fusion reaction. (*b*) PDMP specifically antagonizes one of the actions of BFA. Clearly, PDMP does not act by interference with BFA-induced release of β-COP (Fig. 5). This is consistent with observations from Ivessa et al. (1995), who showed that calcium mobilizing agents that prevent BFA-induced retrograde membrane flow did not interfere with β-COP release. This shows that although BFA-induced dissociation of coatomer from membranes is required for redistribution of Golgi membranes into the ER (Scheel et al., 1997), it is not sufficient. In this respect, it has recently been shown in permeabilized cells that in the absence of NAD^+, BFA can dissociate coatomer from the Golgi complex without affecting the structure of the organelle (Mironov et al., 1997). NAD^+- and BFA-dependent ADP-ribosylation of BARS-50 was shown to play a role in the Golgi disassembling activity of BFA. On the other hand, it cannot be excluded that PDMP (partly) exerts its effect by detoxification of BFA, as has been shown to occur for forskolin (Nickel et al., 1996), an activator of adenylyl cyclase, which also inhibits BFA-induced retrograde membrane flow (Lippincott et al., 1991). However, we consider this possibility unlikely, given the fast kinetics of PDMP action (no preincubation with PDMP is required to obtain inhibition of BFA-induced retrograde membrane flow; even addition of PDMP 3 min after BFA is effective), compared with the kinetics of secretion of BFA conjugates.

In conclusion, PDMP inhibition of BFA-induced retrograde membrane flow in the ER/Golgi system is dissociated from its well-known effect on glycosphingolipid metabolism and does not involve direct interference with the integrity of Golgi membranes. Rather, it appears to be related to specific modulation of calcium homeostasis, a novel action of the drug, and mimicked by a specific antagonist of the MRP pump. Thus, PDMP is a novel tool to interfere with BFA-induced retrograde Golgi to ER membrane transport and provides new insights into the physiological mechanisms underlying this process. Future work will aim at further identification of PDMP-sensitive calcium pools and the assessment of the role of these pools and calcium influx inhibition in membrane transport between Golgi and ER. Furthermore, we will investigate whether the effects of PDMP on BFA-induced retrograde membrane transport are a reflection of inhibition of retrograde transport under physiological circumstances (e.g., without BFA).

The authors thank Jacqueline Plass and Coen Wiegman for their contribution to the initial observations on PDMP inhibition of BFA-induced retrograde membrane transport, Han Roelofsen for his help with confocal scanning laser microscopy, and Peter van der Syde for the skillful technical assistance in photo-editing/printing.

The research of Jan Willem Kok has been made possible by a fellowship of the Royal Netherlands Academy of Arts and Sciences (KNAW). Teresa Babia was supported by a grant from the Comissio Interdepartamental de Recerca i Innovacio Tecnologia. Gustavo Egea was supported by a grant from the Comissio Interdepartamental de Ciencia y Tecnologia (SAF 97/0016). Catalin M. Filipeanu is a recipient of an Ubbo Emmius fellowship from the Groningen Utrecht Institute for Drug Exploration.

Received for publication 9 December 1997 and in revised form 27 May 1998.

References

Alcalde, J., P. Bonay, A. Roa, S. Vilaro, and I.V. Sandoval. 1992. Assembly and disassembly of the Golgi complex: two processes arranged in a *cis-trans* direction. *J. Cell Biol.* 116:69–83.

Alcalde, J., G. Egea, and I.V. Sandoval. 1994. gp74, a membrane glycoprotein of the *cis*-Golgi network that cycles through the endoplasmic reticulum and intermediate compartment. *J. Cell Biol.* 124:649–665.

Aridor, M., and W.E. Balch. 1996. Principles of selective transport: coat complexes hold the key. *Trends Cell Biol.* 8:315–320.

Bednarek, S.Y., L. Orci, and R. Schekman. 1996. Traffic COPs and the formation of vesicles. *Trends Cell Biol.* 6:468–473.

Bligh, E.G., and W.J. Dyer. 1959. A rapid method of total lipid extraction and purification. *Can. J. Biochem. Physiol.* 37:911–917.

Böttcher, C.J.F., C.M. van Gent, and C. Pries. 1961. A rapid and sensitive submicro phosphorus determination. *Anal. Chim. Acta.* 24:203–204.

Cole, N.B., J. Ellenberg, J. Song, D. DiEuliis, and J. Lippincott-Schwartz. 1998. Retrograde transport of Golgi-localized proteins to the ER. *J. Cell Biol.* 140: 1–15.

Donaldson, J.G., D. Cassel, A. Kahn, and R.D. Klausner. 1992. ADP-ribosylation factor, a small GTP-binding protein, is required for binding of the coatomer protein β-COP to Golgi membranes. *Proc. Natl. Acad. Sci. USA.* 89:6408–6412.

Elazar, Z., L. Orci, J. Ostermann, M. Amherdt, G. Tanigawa, and J.E. Rothman. 1994. ADP-ribosylation factor and coatomer couple fusion to vesicle budding. *J. Cell Biol.* 124:415–424.

Filipeanu, C.M., D. de Zeeuw, and S.A. Nelemans. 1997. Δ^9-Tetrahydrocannabinol activates $[Ca^{2+}]_i$ increases partly sensitive to capacitative store refilling. *Eur. J. Pharmacol.* 336:R1– R3.

Friche, E., P.B. Jensen, and N.I. Nissen. 1992. Comparison of cyclosporin A and SDZ PSC833 as multidrug-resistance modulators in a daunorubicin-resistant Ehrlich ascites tumor. *Cancer Chemother. Pharmacol.* 30:235–237.

Gekeler, V., W. Ise, K.H. Sanders, W.-R. Ulrich, and J. Beck. 1995. The leukotriene LTD_4 receptor antagonist MK571 specifically modulates MRP associated multidrug resistance. *Biochem. Biophys. Res. Commun.* 208:345–352.

Grynkiewicz, G., M. Poenie, and R.Y. Tsien 1985. A new generation of Ca^{2+} indicators with greatly improved fluorescence properties. *J. Biol. Chem.* 260: 3440–3450.

Helms, J.B., and J.E. Rothman. 1992. Inhibition by brefeldin A of a Golgi membrane enzyme that catalyzes exchange of guanine nucleotide bound to ARF. *Nature (Lond.).* 360:352–354.

Ivessa, N.E., C. De Lemos-Chiarandini, D. Gravotta, D.D. Sabatini, and G. Kreibich. 1995. The brefeldin A-induced retrograde transport from the Golgi apparatus to the endoplasmic reticulum depends on calcium sequestered to intracellular stores. *J. Biol. Chem.* 270:25960– 25967.

Johannes, L., D. Tenza, C. Antony, and B. Goud. 1997. Retrograde transport of KDEL-bearing B-fragment of Shiga toxin. *J. Biol. Chem.* 272:19554–19561.

Klausner, R.D., J.G. Donaldson, and S.J. Lippincott. 1992. Brefeldin A: insights into the control of membrane traffic and organelle structure. *J. Cell Biol.* 116:1071–1080.

Kok, J.W., and D. Hoekstra. 1993. Fluorescent lipid analogues. Applications in cell- and membrane biology. *In* Fluorescent Probes for Biological Function of Living Cells. A Practical Guide. W.T. Mason and G. Relf, editors. Academic Press, London. 100–119.

Kok, J.W., K. Hoekstra, S. Eskelinen, and D. Hoekstra. 1992. Recycling pathways of glucosylceramide in BHK cells: distinct involvement of early and late endosomes. *J. Cell Sci.* 103:1139–1152.

Kok, J.W., T. Babia, K. Klappe, and D. Hoekstra. 1995. Fluorescent, short-chain C_6-NBD- sphingomyelin, but not C_6-NBD-glucosylceramide, is subject to extensive degradation in the plasma membrane: implications for signal transduction related to cell differentiation. *Biochem. J.* 309:905–912.

Lavie, Y., H. Cao, S.L. Bursten, A.E. Giuliano, and M.C. Cabot. 1996. Accumulation of glucosylceramides in multidrug-resistant cancer cells. *J. Biol. Chem.* 271:19530–19536.

Lavie, Y., H. Cao, A. Volner, A. Lucci, T-Y. Han, V. Geffen, A.E. Giuliano, and M.C. Cabot. 1997. Agents that reverse multidrug resistance, tamoxifen, verapamil, and cyclosporin A, block glycosphingolipid metabolism by inhibiting ceramide glycosylation in human cancer cells. *J. Biol. Chem.* 272:1682–1687.

Lippincott, S.J., L.C. Yuan, J.S. Bonifacino, and R.D. Klausner. 1989. Rapid redistribution of Golgi proteins into the ER in cells treated with brefeldin A: evidence for membrane cycling from Golgi to ER. *Cell.* 56:801–813.

Lippincott, S.J., J. Glickman, J.G. Donaldson, J. Robbins, T.E. Kreis, K.B. Seamon, M.P. Sheetz, and R.D. Klausner. 1991. Forskolin inhibits and reverses the effect of brefeldin A on Golgi morphology by a cAMP-independent mechanism. *J. Cell Biol.* 112:567–577.

Lipsky, N.G., and R.E. Pagano. 1985. A vital stain for the Golgi apparatus. *Science.* 228:745–747.

Liu, P.S., M.Y. Ho, and H.L. Hsieh. 1996. Effects of extracellular ATP on Ca^{2+} mobilization in Madin Darby canine kidney (MDCK) cells. *Clin. J. Physiol.* 39:189–196.

Lytton, J., M. Westlin, and M.R. Hanley. 1991. Thapsigargin inhibits the sarcoplasmic or endoplasmic reticulum Ca^{2+}-ATPase family of calcium pumps. *J. Biol. Chem.* 266:17067–17071.

Maceyka, M., and C.E. Machamer. 1997. Ceramide accumulation uncovers a cycling pathway for the *cis*-Golgi network marker, infectious bronchitis virus M protein. *J. Cell Biol.* 139:1411–1418.

McIntyre, J.C., and R.G. Sleight. 1991. Fluorescence assay for phospholipid membrane asymmetry. *Biochemistry.* 30:11819–11827.

Mironov, A., A. Colanzi, M.G. Silletta, G. Fiucci, S. Flati, A. Fusella, R. Polishchuk, A. Mironov, Jr., G. Di Tullio, R. Weigert, et al. 1997. Role of NAD^+ and ADP-ribosylation in the maintenance of the Golgi structure. *J. Cell Biol.* 139:1109–1118.

Nickel, W., J.B. Helms, R.E. Kneusel, and F.T. Wieland. 1996. Forskolin stimulates detoxification of brefeldin A. *J. Biol. Chem.* 271:15870–15873.

Nitschke, R., J. Leipziger, and R. Greger. 1993. Agonist-induced intracellular Ca^{2+} transients in HT29 cells. *Pflugers Arch.* 423:519–526.

Pagano, R.E. 1989. A fluorescent derivative of ceramide: physical properties and use in studying the Golgi apparatus of animal cells. *Methods Cell Biol.* 29:75–85.

Pagano, R.E., O.C. Martin, H.C. Kang, and R.P Haughland. 1991. A novel fluorescent ceramide analogue for studying membrane traffic in animal cells: accumulation at the Golgi apparatus results in altered spectral properties of the sphingolipid precursor. *J. Cell Biol.* 11:1267–1279.

Pizzo, P., C. Fasolato, and T. Pozzan. 1997. Dynamic properties of an inositol-1,4,5-trisphosphate and thapsigargin insensitive calcium pool in mammalian cells. *J. Cell Biol.* 136:355–366.

Radin, N.S., J.A. Shayman, and J. Inokuchi. 1993. Metabolic and functional effects of inhibiting glucosylceramide synthesis with PDMP and other substances. *Adv. Lipid. Res.* 26:183–213.

Rosenwald, A.G., and R.E. Pagano. 1993. Inhibition of glycoprotein traffic through the secretory pathway by ceramide. *J. Biol. Chem.* 268:4577–4579.

Rosenwald, A.G., and R.E. Pagano. 1994. Effects of the glucosphingolipid synthesis inhibitor, PDMP, on lysosomes in cultured cells. *J. Lipid Res.* 35:1232–1240.

Rosenwald, A.G., C.E. Machamer, and R.E. Pagano. 1992. Effects of a sphingolipid synthesis inhibitor on membrane transport through the secretory pathway. *Biochemistry.* 31:3581–3590.

Salter, M.W., and J.L. Hicks. 1995. ATP causes release of intracellular Ca^{2+} via the phospholipase C β/IP_3 pathway in astrocytes from the dorsal spinal cord. *J. Neurosci.* 15:2961–2971.

Scheel, J., R. Pepperkok, M. Lowe, G. Griffiths, and T.E. Kreis. 1997. Dissociation of coatomer from membranes is required for brefeldin A–induced transfer of Golgi enzymes to the endoplasmic reticulum. *J. Cell Biol.* 137:319–333.

Sciaky, N., J. Presley, C. Smith, K.J.M. Zaal, N. Cole, J.E. Moreira, M. Terasaki, E. Siggia, and J. Lippincott-Schwartz. 1997. Golgi tubule traffic and the effects of brefeldin A visualized in living cells. *J. Cell Biol.* 139:1137–1155.

Sipma, H., M. Duin, B. Hoiting, A. den Hertog, and A. Nelemans. 1995. Regulation of histamine- and UTP-induced increases in Ins(1,4,5)P_3, Ins(1,3,4,5)P_4, and Ca^{2+} by cyclic AMP in DDT_1MF-2 smooth muscle cells. *Br. J. Pharmacol.* 114:383–390.

Tanigawa, G., L.Orci, M. Amherdt, J.B. Helms, and J.E. Rothman. 1993. Hydrolysis of bound GTP by ARF protein triggers uncoating of Golgi-derived COP-coated vesicles. *J. Cell Biol.* 123:1365–1371.

Watanabe, T., H. Tsuge, T. Oh-hara, M. Naito, and T. Tsuruo. 1995. Comparative study on reversal efficacy of SDZ PSC833, cyclosporin A and verapamil on multidrug resistance in vitro and in vivo. *Acta Oncologica.* 34:235–241.

Zhang, W., and G.M. Roomans. 1997. Regulation of ion transport by P2u purinoceptors and alpha 2A adrenoceptors in HT29 cells. *Cell Biol. Int.* 21: 195–200.